Periostin modulates extracellular matrix behavior in tendons

Kevin I. Rolnick [a], Joshua A. Choe [a], Ellen M. Leiferman [a], Jaclyn Kondratko-Mittnacht [a], Anna E. B. Clements [a], Geoffrey S. Baer [a], Peng Jiang [b,c], Ray Vanderby [a] and Connie S. Chamberlain [a]*

***a* - Department of Orthopedics and Rehabilitation,** *University of Wisconsin, Madison, WI 53705, USA*
***b* - Center for Gene Regulation in Health and Disease (GRHD) and Department of Biological,** *Geological and Environmental Sciences, Cleveland State University, Cleveland, OH 44115, USA*
***c* - Center for RNA Science and Therapeutics,** *School of Medicine, Case Western Reserve University, Cleveland, OH 44106, USA*

Correspondence to Connie S. Chamberlain:*Dept. of Orthopedics and Rehabilitation, 1111 Highland Ave., WIMR Room 5057, University of Wisconsin, Madison, WI 53705, USA. *Chamberlain@ortho.wisc.edu (C.S. Chamberlain)*
https://doi.org/10.1016/j.mbplus.2022.100124

Abstract

Periostin, originally named osteoblast-specific factor 2 (OSF-2) has been identified primarily in collagen rich, biomechanically active tissues where its role has been implicated in mechanisms to maintain the extracellular matrix (ECM), including collagen fibrillogenesis and crosslinking. It is well documented that periostin plays a role in wound healing and scar formation after injury, in part, by promoting cell proliferation, myofibroblast differentiation, and/or collagen fibrillogenesis. Given the significance of periostin in other scar forming models, we hypothesized that periostin will influence Achilles tendon healing by modulating ECM production. Therefore, the objective of this study was to elucidate the effects of periostin during Achilles tendon healing using periostin homozygous (*Postn*$^{-/-}$) and heterozygous (*Postn*$^{+/-}$) mouse models. A second experiment was included to further examine the influence of periostin on collagen composition and function using intact dorsal tail tendons. Overall, *Postn*$^{-/-}$ and *Postn*$^{+/-}$ Achilles tendons exhibited impaired healing as demonstrated by delayed wound closure, increased type III collagen production, decreased cell proliferation, and reduced tensile strength. Periostin ablation also reduced tensile strength and stiffness, and altered collagen fibril distribution in the intact dorsal tail tendons. Achilles tendon outcomes support our hypothesis that periostin influences healing, while tail tendon results indicate that periostin also affects ECM morphology and behavior in mouse tendons.

Introduction

Rupture of the Achilles tendon is a common injury in North America with a mean incidence of 8.3 per 100,000 people.[1] The healing process can protract years, producing a fibrotic tissue with impaired mechanical properties. Despite new surgical techniques and other therapeutic advancements designed to improve tendon healing, none eliminate scar formation, thereby making them prone to further re-rupture.[2,3] A mechanism to accelerate wound healing and/or reduce scar formation could reduce the likelihood of re-injury and time spent recovering.

Periostin, originally named osteoblast-specific factor 2 (OSF-2) is a nonstructural ECM matricellular protein able to modify cell behavior and biomechanical properties of collagenous-based tissues. It is induced and secreted by activated fibroblasts and myofibroblasts in areas

of tissue injury where it accumulates within the ECM to facilitate type I collagen maturation and crosslinking. Periostin also plays a role in maintaining ECM homeostasis through interactions with proteins including tenascin-C and fibronectin.

It is well documented that periostin plays a role in wound healing and scar formation after injury, in part, by promoting cell proliferation, myofibroblast differentiation, and/or collagen fibrillogenesis. [3–10] Within skin wounds, periostin is upregulated after injury and peaks 7 days later.[11,12] Similarly, periostin is increased after myocardial infarction and is required for proper scar formation. Previously, we reported the upregulation of periostin within the medial collateral ligament (MCL) and Achilles tendon during early healing.[13,14] The increase in periostin production coincided with upregulated type III collagen, thereby supporting a role in scar formation.[14].

Studies using *Postn* null (*Postn*$^{-/-}$) mice have further supported its role in healing and scar formation. After injury, *Postn*$^{-/-}$ mice had impaired skin wound closures and a reduced population of myofibroblasts typically present at the wound borders.[4] Exogenous delivery of periostin to the *Postn*$^{-/-}$mice, returned myofibroblast presence within the granulation tissue.[11] *Postn*$^{-/-}$ mice also exhibited impaired healing after acute myocardial infarction which resulted from cardiac rupture as a consequence of reduced myocardial stiffness, fewer myofibroblasts, and impaired collagen fibril formation.[5].

Given the significance of periostin in other scar forming models, we hypothesized that periostin will influence Achilles tendon healing by modulating ECM production. Therefore, the objective of the present study was to elucidate the effects of periostin during Achilles tendon healing using periostin homozygous knockout (*Postn*$^{-/-}$) and heterozygous (*Postn*$^{+/-}$) mouse models. A second experiment was included to further examine the influence of periostin on collagen composition and function using intact mouse dorsal tail tendons.

Results

Achilles tendon results

Achilles Tendon Mechanical Testing. To determine if periostin affected tendon function, the intact, day 14-, and day 28-post-injured wild type (WT), *Postn*$^{+/-}$, and *Postn*$^{-/-}$ tendons were mechanically tested. Intact tendons failed primarily at the calcaneal insertion (93%) and to a lesser extent the musculo-tendinous junction (MTJ; 7 %). Failure of the injured tendons occurred at the midsubstance (40.7 %), calcaneal insertion (55.9 %) and MTJ (3.4 %). Mechanical results indicated that the ultimate load of intact tendons was significantly lower in *Postn*$^{+/-}$ tendons compared to the intact WT samples; no differences were noted by the intact *Postn*$^{-/-}$ tendons (Fig. 1**A, G**). Within the healing tendon, ultimate load at day 28 post-injury was lower in the *Postn*$^{-/-}$ tendons compared to the injured WT tendons. No other differences in ultimate load were noted (Fig. 1**A, G**). Ultimate stress was significantly lower in intact *Postn*$^{+/-}$ tendons compared to *Postn*$^{-/-}$ tendons. No differences were noted in ultimate stress after tendon injury (Fig. 1**B, G**). In contrast, ultimate strain was significantly reduced within the *Postn*$^{+/-}$ and *Postn*$^{-/-}$ tendons 28 days post-injury compared to WT samples (Fig. 1**C, G**). No other significant genotype differences were noted in modulus, stiffness, or cross sectional area (Fig. 1**C-G**). As expected, a day effect was noted in all metrics tested, except strain, regardless of genotype; day 28 and/or day 14 tendons were significantly weaker than the intact tendons **(**Fig. 1**F**).

Achilles Tendon Immunohistochemistry. IHC was performed to examine the effects of periostin on tendon cell number and ECM production. To first confirm that *Postn*$^{-/-}$ was abrogated within the *Postn*$^{-/-}$ tissue, tendons were stained for periostin. Very little/no periostin was evident in intact tendons, regardless of genotype (**Supp.** Fig. 1**)**. Injured tendons collected at days 7, 14, and 28 were positive for periostin within both the WT and *Postn*$^{+/-}$ tendons. In contrast, very low/no periostin was detected in the injured *Postn*$^{-/-}$ tendons. Ki67, a marker of proliferating cells, was significantly decreased over time from day 7 to day 28 post-injury, regardless of genotype (Fig. 2**A-B)**. Proliferating cells were also significantly different within the injured tendon based on genotype; *Postn*$^{-/-}$ tendons collected at 7 days post-injury contained fewer proliferating cells compared to the WT tendons. In contrast, more cells were present within the day 14 *Postn*$^{-/-}$ tendons compared to the WT tendons. (Fig. 2**C**). No other differences were noted. Myofibroblasts, a marker of scar formation, were reduced over time within the injured tendon, regardless of genotype (Fig. 2**D-E)**. Further analysis indicated that myofibroblasts were significantly higher within the *Postn*$^{+/-}$ tendons compared to the *Postn*$^{-/-}$ tendons at 7 days post-injury **(**Fig. 2**F)**. To note, the number of myofibroblasts remained similar across time within the *Postn*$^{-/-}$ tendons but were significantly reduced over time within the day 14 *Postn*$^{+/-}$ and day 28 wt samples. Type I collagen, a marker for native tendon, was reduced at 7 days post-injury compared to days 14 and 28, regardless of genotype (Fig. 2**G-H**). No other changes were noted in type I collagen **(**Fig. 2**I).** Type III collagen, another marker of scar formation, was significantly increased from day 7 to day 28 during healing, regardless of genotype **(**Fig. 2**J-K)**. Differences were also noted between genotypes. Type III

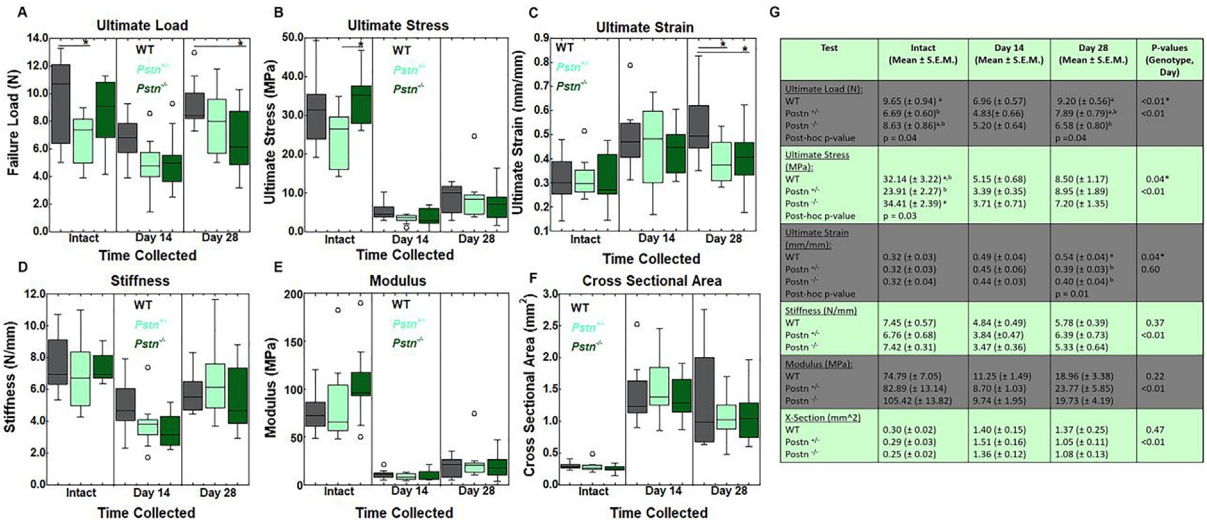

G

Test	Intact (Mean ± S.E.M.)	Day 14 (Mean ± S.E.M.)	Day 28 (Mean ± S.E.M.)	P-values (Genotype, Day)
Ultimate Load (N):				
WT	9.65 (± 0.94) *	6.96 (± 0.57)	9.20 (± 0.56)[a]	<0.01*
Postn +/-	6.69 (± 0.60)[b]	4.83(± 0.66)	7.89 (± 0.79)[a,b]	<0.01
Postn -/-	8.63 (± 0.86)[a,b]	5.20 (± 0.64)	6.58 (± 0.80)[b]	
Post-hoc p-value	p = 0.04		p =0.04	
Ultimate Stress (MPa):				
WT	32.14 (± 3.22)[a,b]	5.15 (± 0.68)	8.50 (± 1.17)	0.04*
Postn +/-	23.91 (± 2.27)[b]	3.39 (± 0.35)	8.95 (± 1.89)	<0.01
Postn -/-	34.41 (± 2.39)*	3.71 (± 0.71)	7.20 (± 1.35)	
Post-hoc p-value	p = 0.03			
Ultimate Strain (mm/mm):				
WT	0.32 (± 0.03)	0.49 (± 0.04)	0.54 (± 0.04)*	0.04*
Postn +/-	0.32 (± 0.03)	0.45 (± 0.06)	0.39 (± 0.03)[b]	0.60
Postn -/-	0.32 (± 0.04)	0.44 (± 0.03)	0.40 (± 0.04)[b]	
Post-hoc p-value			p = 0.01	
Stiffness (N/mm)				
WT	7.45 (± 0.57)	4.84 (± 0.49)	5.78 (± 0.39)	0.37
Postn +/-	6.76 (± 0.68)	3.84 (±0.47)	6.39 (± 0.73)	<0.01
Postn -/-	7.42 (± 0.31)	3.47 (± 0.36)	5.33 (± 0.64)	
Modulus (MPa):				
WT	74.79 (± 7.05)	11.25 (± 1.49)	18.96 (± 3.38)	0.22
Postn +/-	82.89 (± 13.14)	8.70 (± 1.03)	23.77 (± 5.85)	<0.01
Postn -/-	105.42 (± 13.82)	9.74 (± 1.95)	19.73 (± 4.19)	
X-Section (mm^2)				
WT	0.30 (± 0.02)	1.40 (± 0.15)	1.37 (± 0.25)	0.47
Postn +/-	0.29 (± 0.03)	1.51 (± 0.16)	1.05 (± 0.11)	<0.01
Postn -/-	0.25 (± 0.02)	1.36 (± 0.12)	1.08 (± 0.13)	

Fig. 1. Influence of periostin on mechanical properties within the intact and injured Achilles tendons. A) Ultimate load was reduced within intact *Postn*$^{+/-}$ tendons compared to intact WT tendons. Within the day 28 healing tendon, load was significantly lower in *Postn*$^{-/-}$samples compared to WT tendons. No other differences in ultimate load were noted. **B)** Ultimate stress was significantly reduced in intact *Postn*$^{+/-}$ tendons compared to the intact *Postn*$^{-/-}$ tendons. No other differences in ultimate stress were noted. **C)** Ultimate strain was reduced in *Postn*$^{-/-}$ and *Postn*$^{+/-}$ tendons 28 days post-injury compared to WT injured tendons. No significant differences were found in **D)** stiffness, **E)** Young's modulus, or **F)** cross sectional area. **G)** Overview of mechanical properties of Achilles tendon. Data are results of two-way ANOVA. *indicates significant difference between genotype within the day collected of given metric. Significant results in genotype (based on $p \leq 0.05$) were further examined via Tukey's post-hoc analysis, and differences were denoted via superscript (^{a,b}) If superscripts are different (e.g. "a" vs "b", then the groups are statistically different from each other within the given metric. Data are expressed as box plots.

collagen was elevated at days 7, 14, and 28 post-injury within *Postn*$^{-/-}$ tendons compared to the WT and/or *Postn*$^{+/-}$ tendons. While type III collagen localization within *Postn*$^{+/-}$ tendons was similar to WT tendons at days 7 and 14, levels were significantly lower at day 28 post-injury. (Fig. 2**J-L**). Another method to monitor tendon scar formation is via calculating the type I:type III collagen ratio. Regardless of genotype, the type I:type III collagen ratio was reduced over the course of healing from day 7 to day 28 (Fig. 2**M**). The ratio was also different between genotypes. Specifically, type I:III collagen was decreased within the *Postn*$^{+/-}$ and *Postn*$^{-/-}$ tendons compared to the WT samples at 7 days post-injury (Fig. 2**N**). While no changes were noted at day 14, *Postn*$^{+/-}$ tendons remained higher in type I:III collagen compared to the WT and *Postn*$^{-/-}$ at day 28 post-injury. Lastly, CD31, a marker to identify endothelial cells, was significantly decreased from day 7 to day 14 post-injury, regardless of genotype. (Fig. 2**O**). No other changes were noted in endothelial cells **(**Fig. 2**P-Q).**

Achilles Tendon Histology. To examine the effects of periostin on wound size, tendons were stained with H&E, imaged, and wound size was measured. Injury to the Achilles tendon in *Postn*$^{-/-}$ and *Postn*$^{+/-}$ mice, resulted in a larger wound size at days 7 and 14 post-injury compared to the WT tendons. (Fig. 3**A-B**). By day 28, wound size was similar between genotypes.

Tail tendon Results:

Tail Tendon Mechanical Testing. To further explore the effects of periostin on mechanical properties, the mouse dorsal tail tendons were examined between the intact *Postn*$^{-/-}$, *Postn*$^{+/-}$, and WT animals. Intact tail tendons from *Postn*$^{-/-}$ and *Postn*$^{+/-}$ mice exhibited a significant reduction in ultimate load, stiffness, stress, and Young's modulus, compared to WT tendons (Fig. 4**A-D, F**). No differences were noted between the *Postn*$^{-/-}$*and Postn*$^{+/-}$groups. Cross sectional area of the tendons were also not significantly different between groups (Fig. 4**E-F)**.

Tail Tendon TEM. To elucidate the compositional differences between the *Postn*$^{-/-}$ and WT tail tendon fibrils, samples were subjected to TEM. As no differences were noted between the *Postn*$^{-/-}$*and Postn*$^{+/-}$ groups within the mechanical testing results, the *Postn*$^{+/-}$group was omitted from analysis. The overall average diameter of fibrils was not significantly different between the two genotypes (Fig. 5**A, F**). However, when fibrils were grouped according to size, a difference in diameter was noted in large fibrils ranging from 300 to 400 nm. *Postn*$^{-/-}$ fibrils were

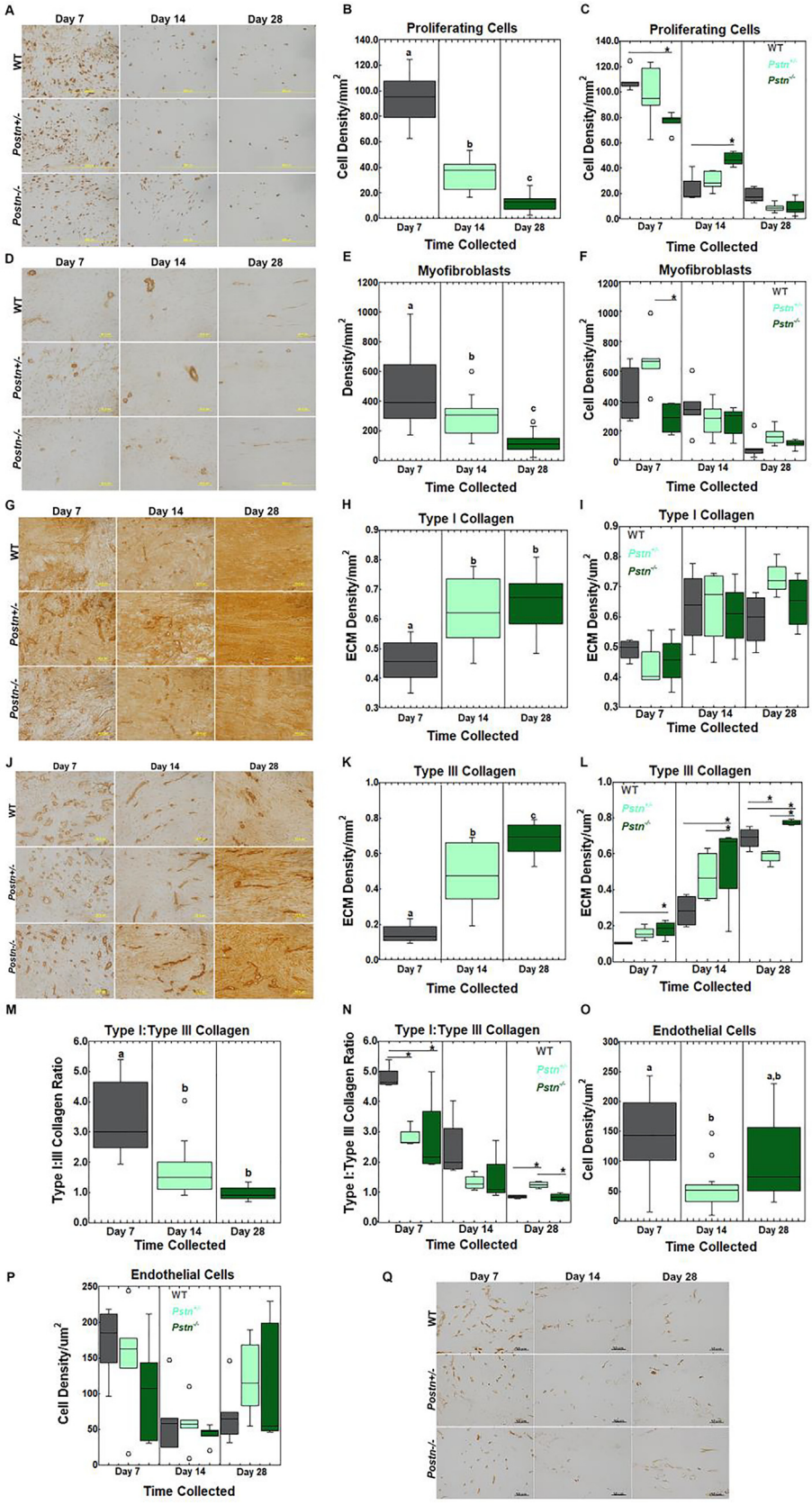
A
Day 7
Day 14
Day 28
WT
Postn+/-
Postn-/-
B
Proliferating Cells
Cell Density/mm2
Time Collected
C
Proliferating Cells
WT
Pstn+/-
Pstn-/-
Cell Density/mm2
Time Collected
D
E
Myofibroblasts
Density/mm2
Time Collected
F
Myofibroblasts
Cell Density/um2
Time Collected
G
H
Type I Collagen
ECM Density/mm2
Time Collected
I
Type I Collagen
ECM Density/um2
Time Collected
J
K
Type III Collagen
ECM Density/mm2
Time Collected
L
Type III Collagen
ECM Density/um2
Time Collected
M
Type I:Type III Collagen
Type I:III Collagen Ratio
Time Collected
N
Type I:Type III Collagen
Type I:Type III Collagen Ratio
Time Collected
O
Endothelial Cells
Cell Density/um2
Time Collected
P
Endothelial Cells
Cell Density/um2
Time Collected
Q

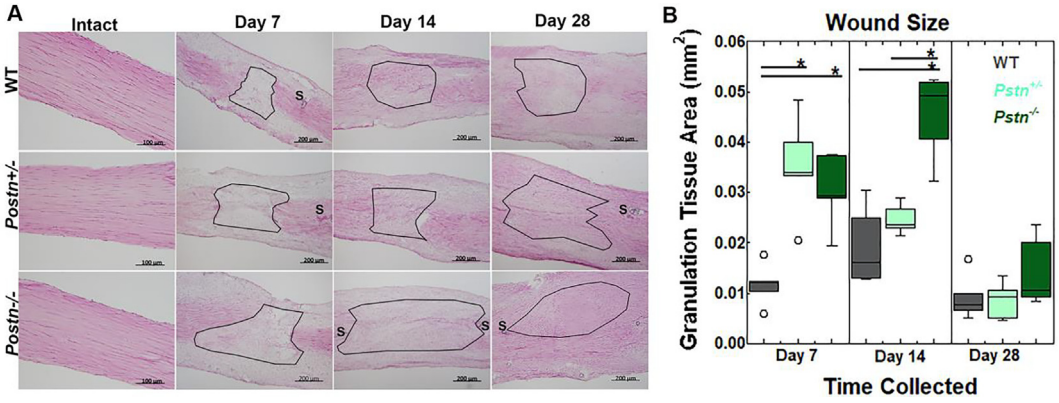

Fig. 3. Wound size of the healing Achilles tendon after injury. A) Representative H&E images of the intact and injured tendons from WT, *Postn*$^{+/-}$, and *Postn*$^{-/-}$ tendons. **B)** Wound size was significantly larger in tendons of *Postn*$^{-/-}$ and *Postn*$^{+/-}$ collected at 7 and 14 days post-injury, compared to WT tendons. By day 28, no significant changes were noted. Data were analyzed via two-way ANOVA. Significant results were further analyzed via Tukey's post hoc analysis. Results are considered significant if $p \leq 0.05$. Data are expressed as box plots.* denote differences between groups. S:suture. Black outlines indicate wound region.

significantly larger compared to the WT tendons (Fig. 5**B-C, F**). Fibril volume fraction analysis indicated *Postn*$^{-/-}$ tendons contained fewer fibrils (and more matrix) compared to the WT fibrils (Fig. 5**D-F)**. Overall, these results indicate that *Postn*$^{-/-}$ tendons contain fewer but larger sized fibrils within a given area compared to the WT tendons, possibly accounting for the reduced mechanical and structural behaviors observed.

Discussion

The goal of this study was to elucidate the role of periostin on tendon behavior using *Postn*$^{-/-}$ and *Postn*$^{+/-}$ mouse models. To our knowledge, this is the first study to report impaired healing by the *Postn*$^{-/-}$ Achilles tendon as demonstrated by delayed wound closure, increased type III collagen production, decreased type I:type III collagen, altered cell proliferation, and reduced tensile strength. Tendon healing from *Postn*$^{+/-}$ tendons was also impacted but with less severity. Intact *Postn*$^{-/-}$ and *Postn*$^{+/-}$ dorsal tail tendons showed reduced tensile strength and stiffness. *Postn*$^{-/-}$ tail tendons also demonstrated abnormal collagen fibril distribution. The localization of periostin has been previously reported in various musculoskeletal systems. Our own studies reported periostin localization within WT Achilles tendons and medial collateral ligaments.[13,14]

Fig. 2. Immunohistochemistry results of the Achilles tendon. A) Representative images of proliferating cells. **B)** Proliferating cells were reduced across time, regardless of genotype. **C)** Proliferating cells were significantly reduced within the *Postn*$^{-/-}$day 7 healing tendons compared to the WT samples. By day 14, proliferating cells were increased within the *Postn*$^{-/-}$ tendons compared to the WT counterparts. **D)** Representative myofibroblasts images of healing tendon. **E)** Myofibroblasts were significantly reduced over time, regardless of genotype. **F)** Within the day 7 healing tendon, myofibroblasts were increased within the *Postn*$^{+/-}$ samples compared to the *Postn*$^{-/-}$ counterparts. **G)** Representative images of type I collagen. **H)** Type I collagen was increased at days 14 and 28, compared to day 7 post-injury, regardless of genotype. **I)** No changes were noted in genotype across time by type I collagen. **J)** Representative images of type III collagen. **K)** Type III collagen was increased over time, regardless of genotype. **L)** Within the day 7, 14, and 28 healing tendon, type III collagen was significantly increased within the *Postn*$^{-/-}$ samples compared to the WT (days 7, 14 and 28) and *Postn*$^{+/-}$ (days 14 and 28) tendons. **M)** Type I:type III collagen was reduced across time, regardless of genotype. **N)** Type I:type III collagen was significantly reduced in the *Postn*$^{-/-}$ and *Postn*$^{+/-}$ tendons at 7 days compared to the WT samples. By day 28 *Postn*$^{+/-}$ tendons were higher in type I:type III collagen compared to the *Postn*$^{-/-}$ and WT samples. **O)** Endothelial cells were reduced within the day 14 healing tendon compared to the day 7 tendon, regardless of genotype. **P)** No changes were noted in endothelial cells across genotype or time of injury. **Q)** Representative images of endothelial cells. Data are results of two-way ANOVA; significant results ($p \leq 0.05$) were further examined via Tukey's post-hoc analysis. Differences across time (**B, E, H, K, M, O)** regardless of genotype are denoted via (^{a,b,c,}). If superscripts are different (e.g. "a" vs "b", then the groups are statistically different from each other within the given metric. Differences in genotype during healing are denoted by *. Data are expressed as box plots.

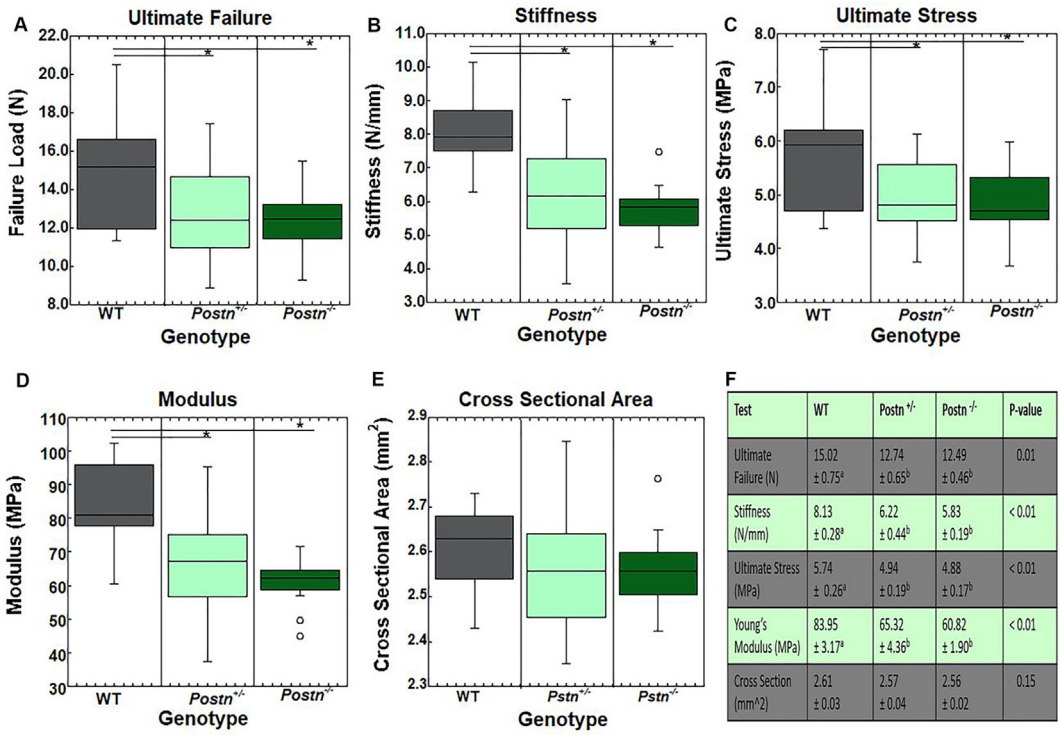

F

Test	WT	Postn +/-	Postn -/-	P-value
Ultimate Failure (N)	15.02 ± 0.75[a]	12.74 ± 0.65[b]	12.49 ± 0.46[b]	0.01
Stiffness (N/mm)	8.13 ± 0.28[a]	6.22 ± 0.44[b]	5.83 ± 0.19[b]	< 0.01
Ultimate Stress (MPa)	5.74 ± 0.26[a]	4.94 ± 0.19[b]	4.88 ± 0.17[b]	< 0.01
Young's Modulus (MPa)	83.95 ± 3.17[a]	65.32 ± 4.36[b]	60.82 ± 1.90[b]	< 0.01
Cross Section (mm^2)	2.61 ± 0.03	2.57 ± 0.04	2.56 ± 0.02	0.15

Fig. 4. Mechanical properties of the intact dorsal tail tendons. Tail tendons from intact *Postn*$^{-/-}$ and *Postn*$^{+/-}$ tendons exhibited lower **A)** ultimate failure **B)** stiffness, **C)** ultimate stress and **D)** Young's modulus compared to the WT tendons. **E)** No changes were noted in cross-sectional area. **F)** Overview of mechanical properties of tail tendons. Data are results of ANOVA. Results are considered significant if $p \leq 0.05$.* denote differences between groups. Data are expressed as box plots.

Within the intact structures, periostin levels are typically low. Injury to these tissues significantly upregulates periostin such that levels are similar to the increases noted with type III collagen. Other labs have reported that fibrocartilage development within the post-natal anterior cruciate ligament (ACL) insertion, is delayed in *Postn*$^{-/-}$ mice.[15] In muscle injury models, *Postn*$^{-/-}$ animals also exhibited a loss of muscle fibers.[16] Combined, these results suggest that periostin plays a significant role in ECM homeostasis and regulation of cell phenotype within the musculoskeletal tissues.

The association of periostin and type I collagen has been well documented in skin and cardiac models.[6,7,10,17,18] Fewer studies have reported correlations between periostin and type I collagen within the tendon. [8,19] In a previous study, we found no association between type I collagen and periostin during normal Achilles tendon healing. [14] However, a concomitant increase in periostin and type III collagen, as well as a decrease in tendon tensile strength was noted.[14] Within the current study, no significant changes in type I collagen were observed within the *Postn*$^{-/-}$ or *Postn*$^{+/-}$ tendons. Unexpectedly, type III collagen was increased within the *Postn*$^{-/-}$ and to a lesser extent, the *Postn*$^{+/-}$ Achilles tendons, which led to a decrease in the type I:type III collagen ratio at day 7. The rationale for the changes in collagen production is unclear but suggests that periostin in part, contributes to controlling the amount of scar that forms. Few studies have reported the influence of periostin on type III collagen behavior during healing. [9,10,20] One study reported that, periostin levels were upregulated within the forming scar of the remodeling tendon, typically dominated with type III collagen. [20] Another study reported that periostin-releasing mesenchymal stromal cells (MSCs) ectopically implanted into a mouse, mediated formation of tendon-like tissue and enhanced type III collagen production.[9] Similarly, periostin levels were positively correlated with type III collagen levels but not type I collagen during chronic cardiac remodeling.[10] Altogether, these results support the concept that periostin influences type III collagen output, although the type of collagen most influenced by periostin may be tissue specific and healing specific.

Periostin modulates cell behavior by inducing cell proliferation and myofibroblast differentiation. [11,12,21] Within the infarcted heart, periostin has been shown to control migration and proliferation of fibroblasts via $\alpha v\beta 3$ which leads to collagen production.[5,17] Periostin is also expressed by fibroblasts and myofibroblasts, cells responsible for production of contractile proteins (such as α-SMA)

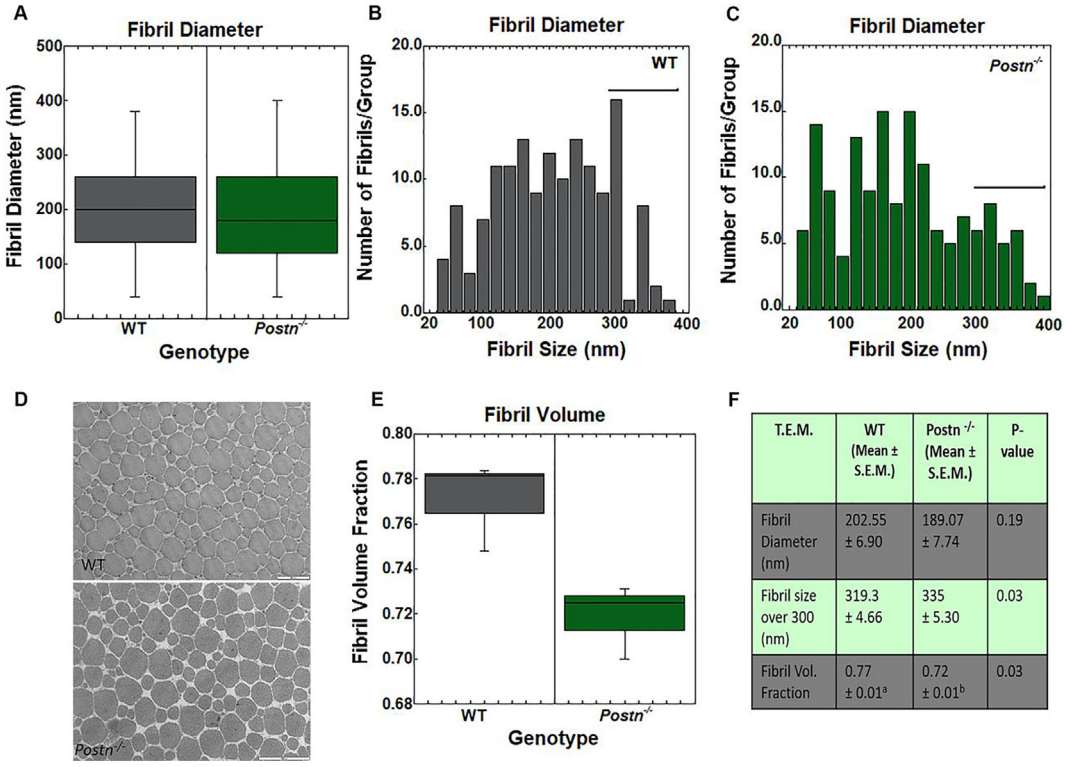

T.E.M.	WT (Mean ± S.E.M.)	Postn -/- (Mean ± S.E.M.)	P-value
Fibril Diameter (nm)	202.55 ± 6.90	189.07 ± 7.74	0.19
Fibril size over 300 (nm)	319.3 ± 4.66	335 ± 5.30	0.03
Fibril Vol. Fraction	0.77 ± 0.01[a]	0.72 ± 0.01[b]	0.03

Fig. 5. TEMresults of the intact dorsal tail tendon fibrils. A) Tail fibril diameters were not significantly different between WT and *Postn*$^{-/-}$ mice. **B-C)** Number of fibrils across varying fibril sizes within the **B)** WT tendons and **C)** *Postn*$^{-/-}$ tendons. Fibrils measuring 300–400 nm were larger in *Postn*$^{-/-}$ tendons vs the WT tendons. **D)** Representative T.E.M. images of WT and *Postn*$^{-/-}$ tail tendons. **E)** Fibril volume fraction was significantly reduced in *Postn*$^{-/-}$ fibrils compared to WT tendons. **F)** Overview of TEM results. Data are results one way ANOVA. Results are considered significant if $p \leq 0.05$. Data are expressed as box plots.

and extracellular matrix proteins (including collagen).[22] In our study, cell proliferation was reduced, and wound repair was delayed by the healing *Postn*$^{-/-}$ Achilles tendons, supporting a beneficial role of periostin in the repair response. While the role of periostin on myofibroblast differentiation has been significantly documented in other healing models, we found only minor temporal differences in myofibroblasts between the WT and *Postn*$^{-/-}$ Achilles tendons. This subtle outcome may be due to the low number of myofibroblasts detected within the healing tendon at the times tested regardless of phenotype. Overall, the reduction in cell populations within the healing *Postn*$^{-/-}$ tendons suggests decreased/delayed wound closure during the early stages of healing.

Aside from modulating cell behavior, periostin may also play a role in collagen fibrillogenesis. In our study, periostin significantly impacted the biomechanical properties of both intact (tail) and healing (Achilles) tendon. While the reduction in tensile strength by the injured *Postn*$^{-/-}$ Achilles tendon partly results from delayed wound repair as indicated by increased wound size, the decrease in biomechanical properties by the intact tail tendons, suggests the differences may lie within the structural composition of the tendon. Indeed a number of reports have demonstrated that collagen fibrillogenesis is altered within the *Postn*$^{-/-}$ tissues, as a reduction in collagen fibril diameter and/or decreased collagen fibril cross-linking was reported [5,8] Our TEM results detected no statistical difference in overall collagen fibril diameter between genotypes. Moreover, fibrils ranging in size from 300 to 400 nm were larger in periostin homozygous animals. While no significant reductions in collagen diameter were detected, there was a significant decrease in tensile strength by the *Postn*$^{-/-}$ tendons. As a decrease in collagen cross-linking can be expected to reduce tensile strength or stiffness, this may partly account for the reduction in tensile strength by the intact *Postn*$^{-/-}$ tail tendons. [6] Our findings also suggest periostin may control collagen fibrillogenesis by altering the amount of type I:type III collagen normally found within the tendon. Indeed, *Postn*$^{-/-}$ Achilles tendons contained significantly reduced ratios of type I:type III collagen compared to the WT tendons. The change in collagen ratio supports the noted reduction in fibril:matrix, and tensile strength by *Postn*$^{-/-}$ intact tendons.

While some similarities in tendon properties were noted between *Postn* heterozygous and homozygous animals, significant discrepancies

were also evident. Within both the *Postn*$^{-/-}$ and *Postn*$^{+/-}$ Achilles tendons, wound size was increased, while type I:type III collagen was decreased after injury. Tensile strength and stiffness were also reduced within the intact *Postn*$^{-/-}$ and *Postn*$^{+/-}$ tail tendons compared to the WT intact tendons. However, IHC results demonstrated that little/no periostin protein was present within the injured homozygous tendons whereas substantial periostin protein was noted within the heterozygous tendons after injury. These results agree with previous reports showing that heterozygous mice continue to produce periostin, albeit at 50–70 % lower levels than WT animals.[23] The lower levels of periostin produced by heterozygous mice, was sufficient to generate discernable differences in tendon dynamics compared to the homozygous tendons. For instance, the delay in Achilles tendon healing was not as severe as the homozygous samples; wound size and type III collagen within the heterozygous tendons were lower by day 14 compared to the homozygous samples. Altogether, these results support a role for periostin during early tendon healing.

This study is not without limitations. While both male and female rodents were included in the study, the animals were randomly assigned to each group creating disproportionate gender numbers within each group. Therefore, sex differences were not analyzed. Second, as we used a global *Postn*$^{-/-}$ mouse model to examine tendon dynamics, gene compensatory mechanisms cannot be ruled out. Periostin is a conserved ECM protein with significant similarities to other family members including βig-h3, stabilin-1, and stabilin-2. The possible compensatory mechanisms of *Bigh3*, *Stab1* and *Stab2* after *Postn* deletion were previously examined [24,25] and a partial overlap of *Postn* with *Bigh3* was detected. However, studies on individual gene disruption of *Postn* and *Bigh3* resulted in distinct phenotypes, suggesting that although the genes are generally similar, there is no tangible evidence to suggest a compensatory mechanism. [26] Lastly, heterozygous tail tendons were not included in the TEM study as the mechanical results indicated no significant differences between the *Postn*$^{-/-}$ and *Postn*$^{+/-}$ tendons.

In conclusion, our results support our hypothesis that periostin can influence Achilles tendon healing by modulating ECM production. These results also suggest that periostin activates cell proliferation and possibly myofibroblast differentiation after tendon injury. The increased cell activity may also promote wound closure. As wound closure progresses, tendon tensile strength and stiffness also improves. Additional studies to elucidate the signaling mechanisms of periostin during tendon healing may aid in identifying molecular targets to accelerate tendon healing and/or reduce scar formation.

Experimental procedures

Animal model

The study was approved by the University of Wisconsin Institutional Animal Use and Care Committee. A total of 165 male and female 8–10 week mice were randomly included in the study. Mouse breeding pairs for B6; 129-*Postn*^{tm1Jmol}/J (strain 009067) were obtained from Jackson Laboratories (Sacramento, CA).[27] *Postn*$^{+/-}$ females were bred with *Postn*$^{-/-}$ males at the University of Wisconsin, Biotron Core. Genotyping of offspring to identify *Postn*$^{-/-}$ mice was performed via Transnetxy (Cordova, TN). C57Bl/6J mice (strain 000664; Jackson Laboratories, Sacramento, CA) were used as the wild type (WT) controls.

To examine the effects of periostin on Achilles tendon healing, a unilateral surgically transected Achilles tendon was used as an experimental model to create a uniform defect for healing as previous described.[28] A total of 55 *Postn*$^{-/-}$, 55 *Postn*$^{+/-}$, and 55 wt mice were included in the study.

Mice were anesthetized using isofluorane. A small, 1 cm skin incision was made over the posterior aspect of the hind limb, distal to the gastrocnemius muscle and proximal to the calcaneus. Underlying fascia was dissected to expose the Achilles tendon. The superficial digital flexor (SDF) tendon was dissected from the Achilles tendon and surgically removed. The Achilles was transected in the midsubstance of the tendon (half way between the calcaneal insertion and the musculotendinous junction) and the tendon ends were repaired using 10–0 suture. The muscular, subcutaneous, and subdermal tissue layers were each closed with 4–0 Dexon suture. The hindlimb was then immobilized using a wire cerclage. All animals were allowed unrestricted cage movement immediately after surgery. Tendons were then collected at 7, 14, or 28 days post-injury and used for immunohistochemistry (IHC; 5 mice/genotype/day) or mechanical testing (10 mice/genotype/day). Tendons designated for IHC were carefully dissected, measured, weighed, and immediately snap-frozen in optimal cutting temperature (OCT) media. Mice used for mechanical testing were stored at −80C until use. A day 7 mechanical group was not included as the tendon is too structurally compromised for meaningful mechanical data. Intact Achilles tendons were also included in the study and used for histology/IHC (n = 10 mice/genotype) and mechanical testing (n = 10 mice/genotype).

Immunohistochemistry/Histology

Immunohistochemistry (IHC) was performed as previously described.[28] Briefly, cryosectioned tendons were fixed with acetone, exposed to 3 %

hydrogen peroxide to eliminate endogenous peroxidase activity, and blocked using Background Buster (Innovex Biosciences, Richmond, CA). Sections were incubated in rabbit polyclonal primary antibodies Ki67 (1:750, Ab15580), CD31 (1:50, Ab28364), alpha-SMA (α-SMA; 1:300, Ab5694), collagen type I (1:800; Ab34710), and collagen type III (1:150; Ab7778), to identify proliferating cells, endothelial cells, myofibroblasts, collagen type I and collagen type III, respectively (all from Abcam, Cambridge, MA). To confirm that that periostin protein was absent in *Postn*$^{-/-}$ samples, a rabbit polyclonal primary antibody for periostin (1:100, PAB16942, Abnova, Walnut, CA) was included. After primary antibody exposure, sections were treated with biotin and streptavidin conjugated to horseradish peroxidase using the StatQ staining kit (Innovex Biosciences). The bound antibody complex was then visualized using diaminobenzidine (DAB). Stained sections were dehydrated with ethanol, cleared, cover-slipped, and viewed under light microscopy. Negative controls omitting the primary antibody were included with each experiment. H&E staining was also performed to measure size of wound region.

Cell counting

Following IHC and H&E staining, images were collected using an Olympus camera-assisted microscope (Nikon Eclipse microscope, model E6000, Mehlville, NY; Olympus model DP79 Center Valley, PA). Three blocked random pictures were obtained from each sample. Images of IHC markers were captured within the healing region. H&E-stained sections were imaged to include the entire healing region, including the borders. Three sections were counted per animal resulting in fifteen sections per genotype per time point. Each captured image was then quantified with ImageJ [29]. For wound healing measurements, wound borders were outlined and the area was quantified via Image J.

Achilles tendon mechanical testing

Mechanical testing was performed to measure the functional effect of periostin on both the intact and healing tendons. Achilles tendons were dissected and the surrounding tissue was excised with care to keep the calcaneal insertion site and the musculotendinous junction (MTJ) intact. Sutures were not removed from the injured tendons based on our previous tests indicating that sutures carried no significant load, and to avoid disruption of the injured region. Tendons remained hydrated via phosphate buffered saline (PBS). Tendon length, width, and thickness were repeatedly measured using digital calipers and the cross-sectional area (assumed to be an ellipse) was estimated. Tendons were tested in a custom-designed load frame, which gripped and loaded the tendons along their longitudinal axis. The calcaneus was trimmed and press-fit into a custom bone grip. The soft tissue end was fixed to strips of Tyvek with a cyanoacrylate adhesive, which were held in a soft-tissue grip. Dimensional measurements for the tendons were recorded at pre-load. Mechanical testing was performed at room temperature. A low preload of 0.1 N was applied in order to obtain a uniform zero point prior to preconditioning (20 cycles at 0.5 Hz) to 0.5 %. Pull-to failure testing was performed on tendons at a rate of 3.33 mm/*sec*. Force and displacement data from the test system were recorded at 10 Hz. Ultimate load was the highest load prior to a complete rupture of the tendon and stress was calculated by dividing the ultimate load by the initial cross-sectional area. Stiffness was calculated as the slope of the most linear portion of the load–displacement curve. Young's modulus was calculated as the slope of the linear portion of the stress–strain curve. Ultimate strain was calculated by dividing tendon deformation by original tendon length.

Tail tendon mechanical testing

A second experiment was performed to examine the effects of periostin on mouse tail tendons. Dorsal tail tendons were obtained from *Postn*$^{-/-}$, *Postn*$^{+/-}$, and WT mice (n = 14 tendons/genotype) initially used for the Achilles tendon healing study. Mechanical testing was completed to compare the functional differences between the *Postn*$^{-/-}$, *Postn*$^{+/-}$, and WT tail tendons. To obtain the tail tendons, the skin was removed to expose the dorsal side tendon. Fascia was carefully cut and tendons were collected. A total of 14 tendons from each genotype (n = 42 total) were tested. Tendon length was measured using a 0–150 mm (0.01 mm resolution) digital caliper. Tendon width and thickness were measured optically using ImageJ (measurements taken at three locations along the tendon length and averaged) and the cross-sectional area (assumed to be an ellipse) was calculated. Tendons were loaded into a mechanical testing frame (Mark-10 Corporation, Copiague, NY), and pulled to failure at 15 mm/min. Load and deformation were recorded, while stiffness, stress, strain, and Young's modulus were calculated as reported above.

Tail tendon transmission electron microscopy (TEM)

Tail dorsal tendons were obtained from *Postn*$^{-/-}$ and WT mice (n = 3 tendons/genotype) initially used for the Achilles tendon healing study. Dorsal tail tendons were fixed in glutaraldehyde and paraformaldehyde. Areas containing collagen bundles were dissected, post-fixed in osmium

tetroxide, dehydrated using a series of graded ethanols, and rinsed in propylene oxide. Samples were then embedded in Spurr's resin. Embedded tendons were cross-sectioned at 70 nm using an ultramicrotome, mounted on 200-mesh copper grids and stained with uranyl acetate and lead citrate. Images were collected from non-overlapping regions of the tendon via Philips CM200 electron microscope (Philips Medical System, Andover, MA) equipped with SIS MegaView 3 digital camera. A total of 9 regions per tendon were obtained. Fibril diameter and distribution were calculated via ImageJ.[29] Fibril volume fraction was calculated according to the American Society of Testing and Materials (ASTM) methods E562-11 for biphasic materials.[30] The ASTM method estimates the volume fraction of an identifiable phase from sections through the microstructure by means of a point grid quantification.

Statistical analysis

A two-way analysis of variance (ANOVA) was used to examine differences between genotypes across time for all Achilles tendon immunohistochemistry and mechanical testing results. IHC staining differences were examined within the healing region. Three replicates per tendon sample (n = 5 samples/day/genotype) were collected and averaged. For each stain, WT and *Postn*$^{+/-}$, *Postn*$^{-/-}$ samples from days 7, 14, and 28 were analyzed for differences in genotype, time, or genotype and time interaction. If the overall p-value was significant, post-hoc comparisons were performed using Tukey's post-hoc test. Tail tendon mechanical results as well as TEM outcomes were examined using one-way ANOVA. $P \leq 0.05$ was used as the criterion for statistical significance. All analyses were performed using KaleidaGraph, version 4.03 (Synergy Software, Inc., Reading, PA).

Funding

Research reported in this publication was supported by the National Institute of Arthritis and Musculoskeletal and Skin Diseases of the National Institutes of Health under Award Number AR059916 and by the AO Foundation under Award Number MSN161649. The content is solely the responsibility of the authors and does not necessarily represent the official views of the AO Foundation or the National Institutes of Health.

CRediT authorship contribution statement

Kevin I. Rolnick : Investigation , Writing – original draft. **Joshua A. Choe :** Investigation , Writing – original draft. **Ellen M. Leiferman :** Investigation. **Jaclyn Kondratko-Mittnacht :** Investigation , Visualization. **Anna E.B. Clements :** Investigation , Visualization . **Geoffrey S. Baer :** Writing – review & editing. **Peng Jiang :** Writing – review & editing. **Ray Vanderby :** Funding acquisition , Resources , Conceptualization , Supervision , Writing - review & editing. **Connie S. Chamberlain :** Conceptualization , Supervision , Visualization , Formal analysis , Data curation , Writing - review & editing .

DATA AVAILABILITY

Data will be made available on request.

DECLARATION OF COMPETING INTEREST

The authors declare that they have no known competing financial interests or personal relationships that could have appeared to influence the work reported in this paper.

Acknowledgements

The authors acknowledge the technical support of Scott Liegel, B.S. and Katherine Klauser, B.S. for IHC and microscopy, and UW-Madison School of Medicine and Public Health TEM facility for TEM work.

Appendix A. Supplementary data

Supplementary data to this article can be found online at https://doi.org/10.1016/j.mbplus.2022.100124.

Received 11 April 2022;
Accepted 3 November 2022;
Available online 9 November 2022

Keywords:
Periostin;
Tendon;
Scar;
Healing;
Collagen;
Wound

Abbreviations:
ANOVA, analysis of variance; DAB, diaminobenzidine; ECM, extracellular matrix; H&E, hematoxylin and eosin; IHC, immunohistochemistry; MCL, medial collateral ligament; MTJ, musculotendinous junction; OCT, optimal cutting temperature; OSF-2, osteoblast specific factor-2; Postn, periostin; SMA, smooth muscle actin; TEM, transmission electron microscopy; WT, wild type

References

[1]. Suchak, A.A., Bostick, G., Reid, D., Blitz, S., Jomha, N., (2005). The incidence of Achilles tendon ruptures in Edmonton. *Canada, Foot Ankle Int*, **26** (11), 932–936.

[2]. Levenson, S.M., Geever, E.F., Crowley, L.V., Oates 3rd, J.F., Berard, C.W., Rosen, H., (1965). The Healing of Rat Skin Wounds. *Ann. Surg.*, **161**, 293–308.

[3]. Lin, T.W., Cardenas, L., Soslowsky, L.J., (2004). Biomechanics of tendon injury and repair. *J. Biomech.*, **37** (6), 865–877.

[4]. Nishiyama, T., Kii, I., Kashima, T.G., Kikuchi, Y., Ohazama, A., Shimazaki, M., Fukayama, M., Kudo, A., (2011). Delayed re-epithelialization in periostin-deficient mice during cutaneous wound healing. *PLoS ONE*, **6** (4), e18410.

[5]. Shimazaki, M., Nakamura, K., Kii, I., Kashima, T., Amizuka, N., Li, M., Saito, M., Fukuda, K., Nishiyama, T., Kitajima, S., Saga, Y., Fukayama, M., Sata, M., Kudo, A., (2008). Periostin is essential for cardiac healing after acute myocardial infarction. *J. Exp. Med.*, **205** (2), 295–303.

[6]. Yang, L., Serada, S., Fujimoto, M., Terao, M., Kotobuki, Y., Kitaba, S., Matsui, S., Kudo, A., Naka, T., Murota, H., Katayama, I., (2012). Periostin facilitates skin sclerosis via PI3K/Akt dependent mechanism in a mouse model of scleroderma. *PLoS ONE*, **7** (7), e41994.

[7]. R.A. Norris, J.D. Potts, M.J. Yost, L. Junor, T. Brooks, H. Tan, S. Hoffman, M.M. Hart, M.J. Kern, B. Damon, R.R. Markwald, R.L. Goodwin, Periostin promotes a fibroblastic lineage pathway in atrioventricular valve progenitor cells, Developmental dynamics : an official publication of the American Association of Anatomists 238(5) (2009) 1052-63.

[8]. Norris, R.A., Damon, B., Mironov, V., Kasyanov, V., Ramamurthi, A., Moreno-Rodriguez, R., Trusk, T., Potts, J.D., Goodwin, R.L., Davis, J., Hoffman, S., Wen, X., Sugi, Y., Kern, C.B., Mjaatvedt, C.H., Turner, D.K., Oka, T., Conway, S.J., Molkentin, J.D., Forgacs, G., Markwald, R.R., (2007). Periostin regulates collagen fibrillogenesis and the biomechanical properties of connective tissues. *J. Cell. Biochem.*, **101** (3), 695–711.

[9]. Noack, S., Seiffart, V., Willbold, E., Laggies, S., Winkel, A., Shahab-Osterloh, S., Florkemeier, T., Hertwig, F., Steinhoff, C., Nuber, U.A., Gross, G., Hoffmann, A., (2014). Periostin secreted by mesenchymal stem cells supports tendon formation in an ectopic mouse model. *Stem Cells Dev*, **23** (16), 1844–1857.

[10]. Minicucci, M.F., Santos, P.P., Rafacho, B.P., Goncalves, A.F., Ardisson, L.P., Batista, D.F., Azevedo, P.S., Polegato, B.F., Okoshi, K., Pereira, E.J., Paiva, S.A., Zornoff, L.A., (2013). Periostin as a modulator of chronic cardiac remodeling after myocardial infarction. *Clinics (Sao Paulo)*, **68** (10), 1344–1349.

[11]. Elliott, C.G., Wang, J., Guo, X., Xu, S.W., Eastwood, M., Guan, J., Leask, A., Conway, S.J., Hamilton, D.W., (2012). Periostin modulates myofibroblast differentiation during full-thickness cutaneous wound repair. *J. Cell Sci.*, **125** (Pt 1), 121–132.

[12]. Ontsuka, K., Kotobuki, Y., Shiraishi, H., Serada, S., Ohta, S., Tanemura, A., Yang, L., Fujimoto, M., Arima, K., Suzuki, S., Murota, H., Toda, S., Kudo, A., Conway, S.J., Narisawa, Y., Katayama, I., Izuhara, K., Naka, T., (2012). Periostin, a matricellular protein, accelerates cutaneous wound repair by activating dermal fibroblasts. *Exp. Dermatol.*, **21** (5), 331–336.

[13]. Chamberlain, C.S., Brounts, S.H., Sterken, D.G., Rolnick, K.I., Baer, G.S., Vanderby, R., (2011). Gene profiling of the rat medial collateral ligament during early healing using microarray analysis. *J. Appl. Physiol.*, **111** (2), 552–565.

[14]. Chamberlain, C.S., Duenwald-Kuehl, S.E., Okotie, G., Brounts, S.H., Baer, G.S., Vanderby, R., (2013). Temporal Healing in Rat Achilles Tendon: Ultrasound Correlations. *Ann. Biomed. Eng.*, **41** (3), 477–487.

[15]. H. Mutsuzaki, K. Kuwahara, H. Nakajima, Influence of periostin on the development of fibrocartilage layers of anterior cruciate ligament insertion, Orthop. Traumatol. Surg. Res. (2022) 103215.

[16]. Ito, N., Miyagoe-Suzuki, Y., Takeda, S., Kudo, A., (2021). Periostin Is Required for the Maintenance of Muscle Fibers during Muscle Regeneration. *Int. J. Mol. Sci.*, **22** (7)

[17]. Kuhn, B., del Monte, F., Hajjar, R.J., Chang, Y.S., Lebeche, D., Arab, S., Keating, M.T., (2007). Periostin induces proliferation of differentiated cardiomyocytes and promotes cardiac repair. *Nat. Med.*, **13** (8), 962–969.

[18]. Yin, S.L., Qin, Z.L., Yang, X., (2020). Role of periostin in skin wound healing and pathologic scar formation. *Chin. Med. J. (Engl)*, **133** (18), 2236–2238.

[19]. Wang, Y., Jin, S., Luo, D., He, D., Shi, C., Zhu, L., Guan, B., Li, Z., Zhang, T., Zhou, Y., Wang, C.Y., Liu, Y., (2021). Functional regeneration and repair of tendons using biomimetic scaffolds loaded with recombinant periostin. *Nat. Commun.*, **12** (1), 1293.

[20]. Best, K.T., Nichols, A.E.C., Knapp, E., Hammert, W.C., Ketonis, C., Jonason, J.H., Awad, H.A., Loiselle, A.E., (2020). NF-kappaB activation persists into the remodeling phase of tendon healing and promotes myofibroblast survival. *Sci. Signal*, **13** (658)

[21]. Crawford, J., Nygard, K., Gan, B.S., O'Gorman, D.B., (2015). Periostin induces fibroblast proliferation and myofibroblast persistence in hypertrophic scarring. *Exp. Dermatol.*, **24** (2), 120–126.

[22]. Kanisicak, O., Khalil, H., Ivey, M.J., Karch, J., Maliken, B. D., Correll, R.N., Brody, M.J., SC, J.L., Aronow, B.J., Tallquist, M.D., Molkentin, J.D., (2016). Genetic lineage tracing defines myofibroblast origin and function in the injured heart. *Nat. Commun.*, **7**, 12260.

[23]. Rios, H., Koushik, S.V., Wang, H., Wang, J., Zhou, H.M., Lindsley, A., Rogers, R., Chen, Z., Maeda, M., Kruzynska-Frejtag, A., Feng, J.Q., Conway, S.J., (2005). periostin null mice exhibit dwarfism, incisor enamel defects, and an early-onset periodontal disease-like phenotype. *Mol. Cell. Biol.*, **25** (24), 11131–11144.

[24]. Lindsley, A., Li, W., Wang, J., Maeda, N., Rogers, R., Conway, S.J., (2005). Comparison of the four mouse fasciclin-containing genes expression patterns during valvuloseptal morphogenesis. *Gene expression patterns : GEP*, **5** (5), 593–600.

[25]. Norris, R.A., Kern, C.B., Wessels, A., Wirrig, E.E., Markwald, R.R., Mjaatvedt, C.H., (2005). Detection of betaig-H3, a TGFbeta induced gene, during cardiac development and its complementary pattern with periostin. *Anat. Embryol.*, **210** (1), 13–23.

[26]. Mosher, D.F., Johansson, M.W., Gillis, M.E., Annis, D.S., (2015). Periostin and TGF-beta-induced protein: Two

peas in a pod? *Crit. Rev. Biochem. Mol. Biol.*, **50** (5), 427–439.

[27]. Oka, T., Xu, J., Kaiser, R.A., Melendez, J., Hambleton, M., Sargent, M.A., Lorts, A., Brunskill, E.W., Dorn 2nd, G. W., Conway, S.J., Aronow, B.J., Robbins, J., Molkentin, J. D., (2007). Genetic manipulation of periostin expression reveals a role in cardiac hypertrophy and ventricular remodeling. *Circ. Res.*, **101** (3), 313–321.

[28]. Chamberlain, C.S., Clements, A.E.B., Kink, J.A., Choi, U., Baer, G.S., Halanski, M.A., Hematti, P., Vanderby, R., (2019). Extracellular Vesicle-Educated Macrophages Promote Early Achilles Tendon Healing. *Stem cells*, **37** (5), 652–662.

[29]. Rasband, W.S., (1997). ImageJ. U.S. National Institutes of Health, Bethesda, Maryland, USA.

[30]. A. International, ASTM E562-19E1: Standard Test Method for Determining Volume Fraction by Systemic Manual Point Count, Annual Book of ASTM Standards2019.